NMR Structural Model of the Interaction of Herbicides with the Photosynthetic Reaction Center from *Rhodobacter sphaeroides*

Nicola D'Amelio,[a] Elena Gaggelli,[a] Piotr Mlynarz,[b] Elena Molteni,[a] Gianni Valensin,*[a] and Wolfgang Lubitz[c]

The interaction of the herbicides acifluorfen and paraquat with the photosynthetic reaction center from Rhodobacter sphaeroides *has been studied by NMR relaxation measurements. Interaction in aqueous solution has been demonstrated by evaluating motional features of the bound form through cross-relaxation terms of protons at fixed distances on the herbicides. Contributions to longitudinal nonselective relaxation rates different from the proton–proton dipolar relaxation were inferred, most probably due to paramagnetic effects originating from the high-spin nonheme Fe^{II} ion in the reaction center. Paramagnetic contributions to proton relaxation rates were converted into distance constraints in order to build a model for the interaction. The models place paraquat in the Q_B site, where most herbicides interact, in agreement with docking calculations, whereas acifluorfen was placed between the metal and the Q_B site, as also demonstrated by the induced paramagnetic shifts. Acifluorfen could therefore act to break the electron-transfer pathway between the Q_A and Q_B sites.*

Introduction

An understanding of the mode of interaction of the photosynthetic reaction center from *Rhodobacter sphaeroides* with herbicides can reveal important information about the mechanism of inhibition of photosynthesis in general, due to the close structural homology of this reaction center with the photosystem II (PSII) complex found in thylakoid membranes of photosynthetic eukaryotes and cyanobacteria.[1] A high-resolution structure of PSII has not yet been determined;[2,3] however, close homologies exist between the D1 and D2 proteins of PSII with two subunits, named L and M, of the bacterial reaction center complex.[4–12] Both the L and M subunits bind the electron donor (special-pair bacteriochlorophylls) and the electron acceptor (quinone–iron complex)[9] of the electron-transfer chain; the quinone site on the L subunit (which binds Q_B) is accessible to a variety of electron-transfer-blocking substances, which can displace Q_B from its binding site.[13–17] On the contrary, Q_A (the quinone on the quinone site of the M subunit) is tightly bound and is more difficult to extract.[1,18] A six-coordinated Fe^{II} ion in a high spin state[16,19,20] is placed between the Q_A and Q_B sites, with the quinone ligands belonging to both the L and M protein subunits. Although direct involvement has not been demonstrated so far, iron removal modifies the kinetics without preventing the electron transfer.[1]

A well-defined Q_B site model has been provided by X-ray diffraction analysis, which shed light on the structure of the intermediates in the reductive reaction cycle.[21,22] In the same way, several investigations have been performed on inhibitors bound to the bacterial reaction center.[13,17,23–26] These inhibitors block the electron transfer from Q_A to Q_B and are widely used as herbicides. A mechanism of competitive inhibitor action at the Q_B site has therefore been proposed. However, it has been noticed[25] that the light-induced formation of Q_A^- enhances the dissociation constant of bound inhibitor; since it is known that the $Q_A^-Q_B \leftrightarrow Q_AQ_B^-$ step moves Q_B from a proximal (closer to Fe^{II}) binding site towards a distal (farther from Fe^{II}) one, the inhibitor can be hypothesized to compete with Q_B at the proximal site.

Here, we report on the interaction of two herbicides, acifluorfen and paraquat, with the bacterial photosynthetic reaction center (BRC) from *Rhodobacter sphaeroides* and show by NMR spectroscopy that the herbicides bind in the vicinity of the Fe^{II} ion and the Q_B site.

Acifluorfen (ACF) is a diphenylether herbicide belonging to the first generation of the family of peroxidizers, which induce inhibition of chlorophyll biosynthesis and photooxidative destruction of plant membranes, thus affecting the photosynthetic pigment content.[27,28] Its interaction with the photosystem II complex has previously been studied.[29–31]

Paraquat (1,1′-dimethyl-4,4′-bipyridinium dichloride, PAR) is the active component of several commercial herbicides that are used to destroy any type of weed. This chemical com-

[a] *Dr. N. D'Amelio, Prof. E. Gaggelli, Dr. E. Molteni, Prof. G. Valensin*
Department of Chemistry and the NMR Center
University of Siena, Via A. Moro, 53100 Siena (Italy)
Fax: (+39) 0577-234254
E-mail: valensin@unisi.it

[b] *Dr. P. Mlynarz*
Faculty of Chemistry, University of Wroclaw
F. Joliot-Curie 14, 50-383 Wroclaw (Poland)
and Faculty of Chemistry, University of Gdansk
80-952 Gdansk (Poland)

[c] *Prof. W. Lubitz*
Max-Planck-Institut für Bioanorganische Chemie
Stiftstrasse 34–36, 45470 Mülheim an der Ruhr (Germany)

 DOI: 10.1002/cbic.200400012

pound is adsorbed very fast on the leaves of any plant and inhibits the photosynthesis process.[32]

Accumulated experience of NMR investigations of medium-size ligands interacting with macromolecules[33–35] and the long-range properties of the paramagnetic effect[36–38] originating from the Fe^{II} ion, the only paramagnetic species in the dark in the BRC, have allowed us to structurally characterize the bound form of the herbicide from study of its fast-exchanging free form and to dock it onto the reaction center.

Results and Discussion

Proton assignment

The ^{1}H NMR spectra of acifluorfen (ACF; 7 mM in D_2O at pH 6.5) and of paraquat (PAR; 6.92 mM in H_2O at pH 6.9), both at 298 K, are shown in Figure 1 together with the molecular structures of the two herbicides. In both cases, protons were named according to their appearance order in the spectrum.

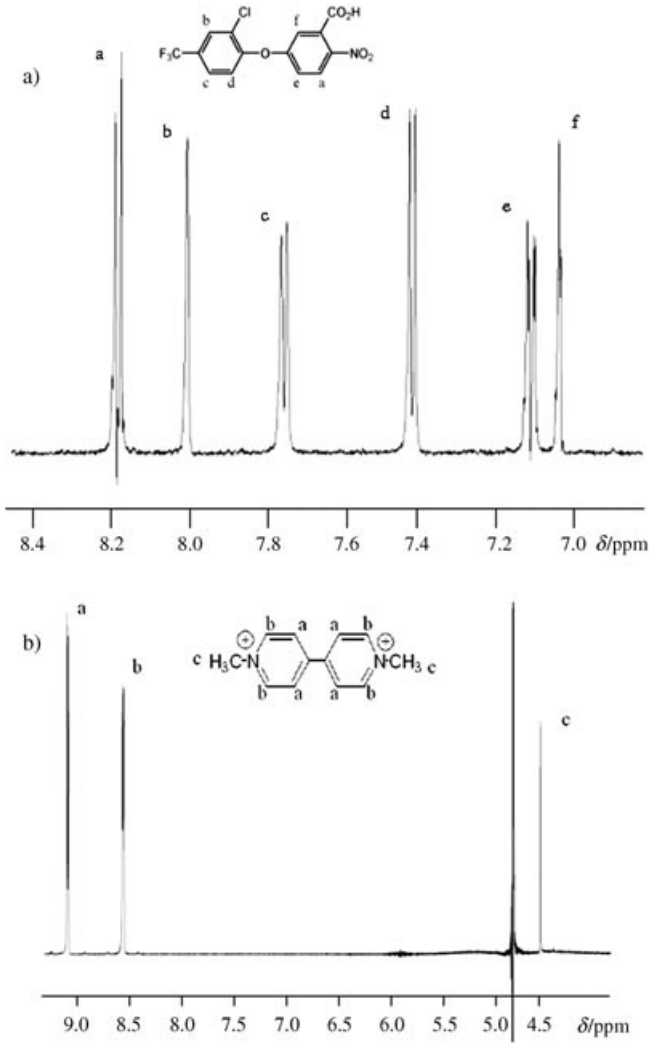

Figure 1. NMR spectra and molecular structures of a) acifluorfen (7 mM in D_2O at pH 6.5) and b) paraquat (6.92 mM in H_2O at pH 6.9), both at 298 K.

The proton assignments for the two molecules are reported in Table 1.

The assignment of signals for paraquat was straightforward, while for acifluorfen it was accomplished by COSY and NOESY 2D spectra (data not shown). An NMR assignment of this herbicide had previously been reported.[39] The differences found for the He and Hf protons are probably due to increased deprotonation of the carboxyl group at the higher pH value used in that report.

Table 1. *^{1}H chemical shifts [ppm] of acifluorfen (7 mM in D_2O at pH 6.5, values uncorrected for the isotopic effect), both free (δ^f) and in the presence of increasing amounts of photosynthetic reaction center from* Rhodobacter sphaeroides *(δ), and of free paraquat (6.92 mM in H_2O at pH 6.9; δ^f). Chemical shifts of acifluorfen bound to the reaction center (δ^b) were calculated by using Equation (1) with the assumption of $x_b = C_{BRC}/C_{ACF}$. $\Delta\delta$ values are the differences between the bound and free values. Missing values refer to protons for which severe overlap caused by broadening prevented the determination.*

Proton	δ^f	$\delta(C_{BRC}:C_{ACF}$ 1:360)	$\delta(C_{BRC}:C_{ACF}$ 1:100)	δ^b	$\Delta\delta$
acifluorfen					
Ha	8.19	8.17	8.10	−2.8	−11.0
Hb	8.01	7.99	7.95	−1.5	−9.5
Hc	7.75	7.74	7.71	−0.3	−8.0
Hd	7.42	7.40	7.38	−0.9	−6.5
He	7.11	7.08	–	−5.9	−13.0
Hf	7.03	7.04	–	–	–
paraquat					
Ha	8.96				
Hb	8.43				
Hc	4.42				

Interaction with the bacterial reaction center

Upon addition of the reaction center to acifluorfen, a severe broadening of lines is observed that increases with the $C_{BRC}:C_{ACF}$ ratio (C = the analytical concentration, Figure 2). We recorded a series of NMR spectra of the herbicide in the presence of BRC ($C_{BRC}:C_{ACF} = 1:180$) at different temperatures (Figure 3), which show that the line broadening is increasing with temperature. Due to the low stability of the reaction center, we could not reach temperatures higher than 303 K. The integrity of the sample was checked after any raise in temperature.

The line broadening suggests interaction of the herbicide with the reaction center, as also ratified by the observed shift (detectable in Figure 2) and enhancement of selective relaxation rates (see below). The temperature dependence of the line broadening strongly supports the idea that the exchange between the free and bound states is approaching the fast-exchange limit ($\tau_M^{-1} > \Delta\tilde{\nu}_{1/2}$) at the higher tested temperatures. In fact, a raise in temperature would, by itself, narrow the line of bound inhibitor, whatever the mechanism of interaction. Exchange between the free and bound forms of acifluorfen slows down by lowering the temperature, thereby making detection of the bound form difficult at low temperature. As the

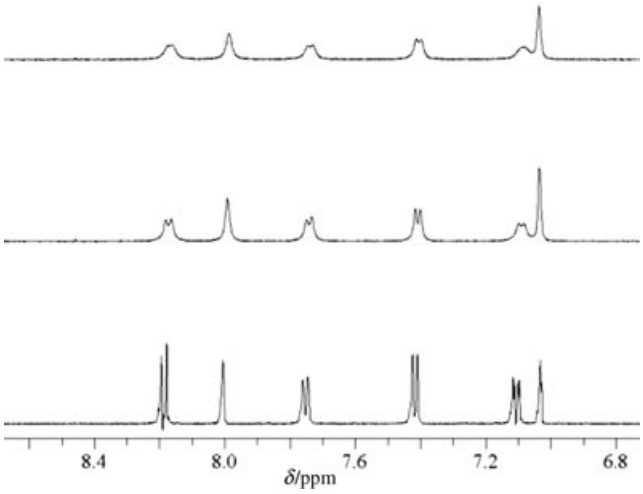

Figure 2. *NMR spectra of acifluorfen (7 mM in D_2O at pH 6.5) at 298 K in the absence (bottom) and presence of BRC in C_{BRC}:C_{ACF} ratios of 1:550 (middle) and 1:365 (top).*

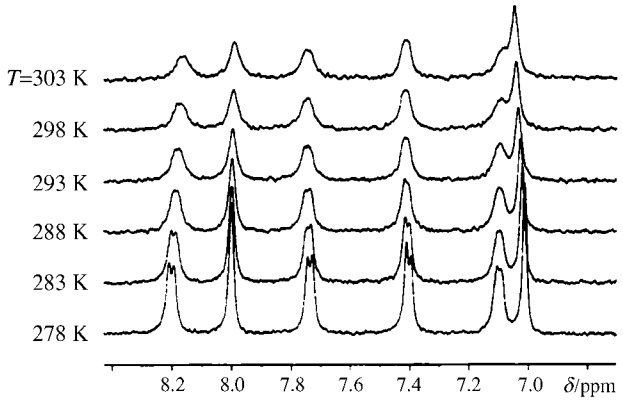

Figure 3. *Temperature dependence of the NMR spectra of acifluorfen (7 mM in D_2O at pH 6.5) obtained in the presence of BRC at a C_{BRC}:C_{ACF} ratio of 1:180.*

exchange is linked to the line width of NMR signals, we can estimate its value to be in the range of milli- to microseconds.

Under fast-exchange conditions, the relationship between NMR parameters in the bound and free forms[33] is described by Equation (1), where *F* refers to a generic NMR parameter, *x* is the molar fraction, f and b subscripts refer to the free and bound states, respectively, obs stands for observed, and τ_M is the exchange time that is the residence time of the molecule in the adduct (the inverse of the 'off rate').

$$F_{obs} = x_f F_f + x_b \frac{1}{F_b^{-1} + \tau_M} \quad (1)$$

Due to the small amount of reaction center and the strength of the interaction (as indicated by the large effect observed on the relaxation rates upon addition of the reaction center in a ratio of 1:550, see Table 2), we can safely assume $x_f \approx 1$ and $x_b = C_{BRC}/C_{herbicide}$. Consequently, parameters of the bound form can be extracted to get insight into the structural and motional features of the interaction.

The value of the molar fraction of bound herbicide was used to estimate the relaxation rates and shifts of the bound form for both herbicides by using Equation (1). (Although paraquat does not display any measurable shift, the relaxation rates were significantly affected.) Relaxation data are shown in Table 2. These values must be considered as lower limits of the "real" value because τ_M was neglected. The change in the values of selective relaxation rates for the free and bound forms reflects the slowing of the reorientational motion caused by the interaction.

The motional correlation time of the bound form, τ_R, was estimated through the Stokes equation [Eq. (2)], where η is the viscosity of the solvent (a value of 8.94×10^{-4} kg m^{-1} s^{-1} based on the viscosity of water[40] was used), r_H is the hydrodynamic radius of the molecule, *k* is the Boltzmann constant, and *T* is the temperature.

$$\tau_R = \frac{4\pi\eta r_H^3}{3kT} \quad (2)$$

The value of r_H is estimated according to Equation (3), where *V* is the specific volume of the reaction center (a value of 0.73×10^{-6} m^3 g^{-1} was used),[41] *M* is the molecular weight (101.8 kDa) of the reaction center, N_A is Avagadro's number, and r_W is the hydration layer (we used a value of 0.16 nm, which corresponds to one half of a hydration shell).[41]

$$r_H = \sqrt[3]{\frac{3VM}{4\pi N_A}} + r_W \quad (3)$$

We obtained a value for the rotational correlation time of 3.12×10^{-8} s. This value nicely agrees with previous measurements.[42]

Table 2. *Nonselective (R_{nsel}), single-selective (R_{sel}), and double-selective (R_{bsel}) relaxation rates of acifluorfen (7 mM in D_2O at pH 6.5, value uncorrected for the isotopic effect) and paraquat (6.92 mM in H_2O at pH 6.9) in the presence (obs superscript) and in the absence (f superscript) of the photosynthetic reaction center from* Rhodobacter sphaeroides*, with a C_{BRC}:$C_{herbicide}$ ratio of 1:550 for acifluorfen and 1:180 for paraquat. Relaxation rates of the two herbicides bound to the reaction center (b superscript) were calculated by using Equation (1) with the assumption that $x_b = C_{BRC}/C_{herbicide}$.*

Proton	R_f^{nsel} [s^{-1}]	R_f^{sel} [s^{-1}]	R_f^{bsel} [s^{-1}]	R_{obs}^{nsel} [s^{-1}]	R_{obs}^{sel} [s^{-1}]	R_{obs}^{bsel} [s^{-1}]	R_b^{nsel} [s^{-1}]	R_b^{sel} [s^{-1}]	R_b^{bsel} [s^{-1}]
acifluorfen									
Ha	0.27	0.22	0.26	0.60	3.62	2.32	182	1874	1135
Hb	0.16	0.16	–	0.52	2.13	–	198	1085	–
Hc	0.34	0.28	0.34	0.61	4.11	2.41	149	2111	1140
Hd	0.33	0.26	0.32	0.61	4.95	2.35	154	2586	1118
He	0.31	0.25	0.29	0.60	4.21	1.94	160	2183	909
Hf	0.15	0.13	–	0.56	2.54	–	226	1327	–
paraquat									
Ha	0.33	0.28	0.32	0.37	0.33	0.36	7.88	10.27	7.96
Hb	0.32	0.29	0.35	0.38	0.36	0.41	10.53	13.59	11.52
Hc	0.65	0.60	–	0.70	0.65	–	11.07	9.49	–

A way to experimentally evaluate the motional correlation time of the bound form is to measure cross-relaxation terms, although they may contain contributions from internal motions and exchange. Cross-relaxation terms were evaluated by the difference of double- and single-selective relaxation rates.[33] Such difference is independent of the occurrence of relaxation mechanisms other than dipolar mechanisms; its functional form, σ, depends on the motional correlation time as described by Equation (4), where R^{bsel} is the double-selective relaxation rate, R^{sel} is the single-selective relaxation rate, μ_0 is the permeability of vacuum, γ is the proton magnetogyric ratio, $\hbar$ is the reduced Planck's constant, r is the interproton distance, ω is the proton Larmor frequency.

$$\sigma = R^{bsel} - R^{bsel} = {}^1/_{10}\left(\frac{\mu_0}{4\pi}\right)^2 \frac{\gamma^4\hbar^2}{r^6}\left(\frac{6\tau_R}{1+4\omega^2\tau_R^2} - \tau_R\right) \quad (4)$$

In the presence of fast exchange, the cross-relaxation terms of the bound form can be extracted from Equation (1). In the case of acifluorfen, the residence time was demonstrated to be rather long (in the range of micro- to milliseconds) and can therefore prevent the measurement of the cross-relaxation rate (F_b^{-1}). For paraquat, the cross-relaxation term between protons at a fixed distance depends uniquely on the motion of the interproton vector (no significant broadening was observed upon addition of the reaction center) and we can measure the correlation time of the motion on both rings by measuring the cross-relaxation rate, σ, of the Ha and Hb protons. The values are reported in Table 3.

Table 3. *Cross-relaxation rates (σ) were measured as the difference between double-selective and single-selective relaxation rates and were used to estimate the correlation time "τ_R from σ" by using Equation (4). Distances from the Fe^{II} ion (r) were calculated through Equation (5), by using the value of τ_R obtained from Stokes' law, $\tau_R = 3.12\times10^{-2}$ μs, for both herbicides (see text for details).*

Proton	Ha	Hb	Hc	Hd	He	Hf
acifluorfen						
r [nm]	0.40	0.39	0.41	0.41	0.41	0.38
paraquat						
σ [s^{-1}]	−2.31	−2.07	–			
"τ_R from σ" [μs]	7.75×10^{-3}	6.94×10^{-3}	–			
r [nm]	0.68	0.65	0.64			

An average value of 7.35×10^{-9} s for τ_R was found for paraquat, a result showing (by comparison with the overall tumbling time calculated above) the presence of significant contribution from internal motion. The fact that the exchange is much faster than with acifluorfen indicates a weaker interaction.

When considering the values of relaxation rates of the bound form (Table 2), it is quite clear that such high values (especially for acifluorfen) cannot be explained only by proton–proton relaxation. Although selective relaxation rates and the line broadening caused by transverse relaxation can be very large due to the slow tumbling rate, nonselective relaxation at this tumbling regime can only be very small (<0.74). Other contributions to this value can arise from other protons on the reaction-center surface brought near by the interaction, but still the values found in Table 2 are difficult to explain if only proton–proton relaxation is considered. (A maximum value of 0.74 was calculated by using the correlation time obtained from Stokes' law and imposing a proton–proton distance of 0.10 nm.)

Most probably, a sizeable effect from paramagnetic relaxation is present due to the high-spin Fe^{II} ion ($S=2$) placed between the L and M protein subunits in an octahedral environment.[16,43] Location of many herbicides near this paramagnetic center has been previously reported.[13] This center has also been shown to have some role in mediating the electron transfer from the ubiquinone in the Q_A site to the one in the Q_B site.[1] A further confirmation of a paramagnetic effect on the herbicide protons in the case of acifluorfen is provided by the proton chemical shifts induced for acifluorfen upon addition of the reaction center (see Table 1). The paramagnetic shift ($\Delta\delta$ in the table) appears to be negative for protons Ha–He. (The shift of the Hf proton is too small to be meaningful.) Since the paramagnetic shift depends on both the distance from the paramagnetic center and the orientation with respect to the magnetic susceptibility tensor,[36] a direct correlation of the position of the protons with respect to the metal is only possible when an independent estimate of the distances is provided. However, the sign of the shifts only depends on the orientation. In our case, we can extract distances from the paramagnetic relaxation rates by using the Solomon and Curie equations[36] (see below). As calculated proton–proton dipolar contributions to nonselective relaxation rates are all very small, nonselective relaxation rates of the bound form reported in Table 2 are a direct measure of paramagnetic contributions. Table 3 contains distances of each proton from the paramagnetic center calculated from Equation (5), where μ_o is the permeability of vacuum, μ_B is the electron Bohr magneton, g_e is the free-electron g factor, γ_I is the proton magnetogyric ratio, S is the spin quantum number of the paramagnetic species, ω_I and ω_S are the proton and electron precession frequencies, respectively, τ_{c1}, τ_{c2}, and τ_c are correlation times, τ_r is the rotational correlation time of the protein, τ_M is the lifetime of the protein–herbicide adduct, and τ_{e1} and τ_{e2} are the longitudinal and transverse electronic relaxation times of the metal ion, respectively. Contact contributions on protein nuclei were considered to be negligible, with the iron center not being directly accessible.

$$R_{dip} = R_{Solomon} + R_{Curie} = {}^2/_{15}\left(\frac{\mu_0}{4\pi}\right)^2 \mu_B^2 g_e^2 \gamma_I^2 (S(S+1))\frac{1}{r^6}$$
$$\left\{\frac{\tau_{c2}}{1+(\omega_I-\omega_S)^2\tau_{c2}^2} + \frac{3\tau_{c1}}{1+\omega_I^2\tau_{c2}^2} + \frac{6\tau_{c2}}{1+(\omega_I+\omega_S)^2\tau_{c2}^2}\right\} \quad (5)$$
$$+ {}^2/_5\left(\frac{\mu_0}{4\pi}\right)^2 \frac{\mu_B^4 g_e^4 \omega_I^2 (S^2(S+1)^2)}{(3kT)^2 r^6}\left\{\frac{3\tau_c}{1+\omega_I^2\tau_c^2}\right\}$$

$$(\tau_{c1})^{-1} = (\tau_{e1})^{-1}+(\tau_r)^{-1}+(\tau_M)^{-1} \quad (6)$$

$$(\tau_{c2})^{-1} = (\tau_{e2})^{-1}+(\tau_r)^{-1}+(\tau_M)^{-1} \quad (7)$$

$$(\tau_c)^{-1} = (\tau_r)^{-1}+(\tau_M)^{-1} \quad (8)$$

As for the determination of the correlation time, in the Solomon part of the equation the electronic relaxation time dominates over the exchange time (which is in the millisecond range for aciflourfen and certainly larger than picoseconds in any case) and the rotational correlation time, since it is much smaller than both. For the Curie part of the equation, the previously calculated motional correlation time of the bound form was used (3.12×10^{-8} s) for both herbicides. We chose to use this value (and not the one extracted from the cross-relaxation rate reported in Table 3 that contains the contribution from internal motions) because the dipolar interaction between the paramagnetic center and each proton of the herbicide is little affected by internal motions. However, the estimation of the correlation time for the Curie contribution to the longitudinal relaxation time is not critical, since for slow motions the Solomon contribution dominates, especially at short distances.

Finally, in the dark, the only paramagnetic species present in the system is the Fe^{II} center that is in the high-spin state and displays electronic relaxation times of 10^{-12}–10^{-13} s.[36] By using these values, the distances of acifluorfen protons from the metal vary quite dramatically; all distances are in the ranges 0.39–0.42 nm with $\tau_{e1}=\tau_{e2}=10^{-12}$ s and 0.31–0.33 nm with $\tau_{e1}=\tau_{e2}=10^{-13}$ s. The second set of distances appears to be too short, with the Fe^{II} ion being hexacoordinated by the protein. For this reason, an electronic relaxation time of 10^{-12} s was used to evaluate the distances reported in Table 3. Due to the presence of exchange on the micro- to millisecond timescale in the case of acifluorfen, paramagnetic contributions ($1/T_1^b$) could be larger than the values indicated by Table 2 (as mentioned before). In cases where the exchange is of the same order of magnitude as the paramagnetic relaxation rates (T_1^b) or larger, the measured paramagnetic contributions are biased and, in particular, values of T_1 shorter than τ_M are leveled off. For this reason, we interpreted the corresponding distances in terms of upper limit restraints. Such restraints were used for structure calculations with the DYANA program[44] (see Materials and Methods for details), with the structure of the reaction center kept as determined by X-ray crystallography.[8] Figure 4 shows some of the conformations thus obtained for acifluorfen.

The calculation places acifluorfen near the metal, although the structures obtained have a high value of target function (a function proportional to the difference between imposed distances and those obtained in the calculated structure), which indicates a difficulty in satisfying the steric criteria (represented in the program by van der Waals violations) together with the imposed distances between the herbicide and the iron center given in the input. This is most probably due to the fact that the protein has been kept fixed in the calculation, with side-chain rearrangements that may be needed for the interaction not being allowed. Indeed, Figure 5, obtained by building the van der Waals surface of the BRC structure, shows that there is some empty space, accessible from outside, in the vicinity of

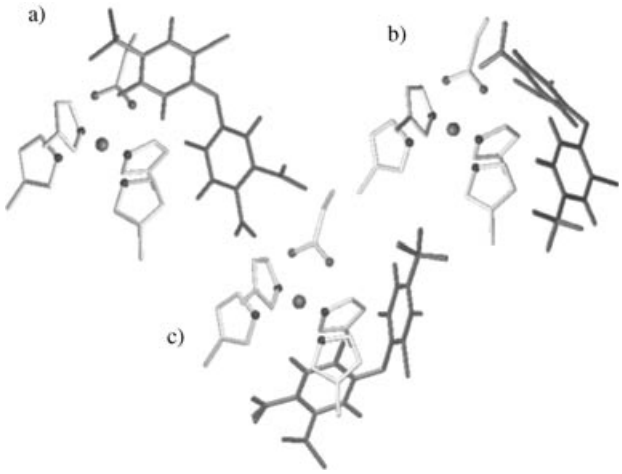

Figure 4. *Possible conformations (within the best five structures) of acifluorfen bound in the BRC as obtained from the DYANA program with the distance restraints in Table 3. The orientation is such that the Q_A and Q_B quinone sites (not shown) are on the left and right of the iron center, respectively.*

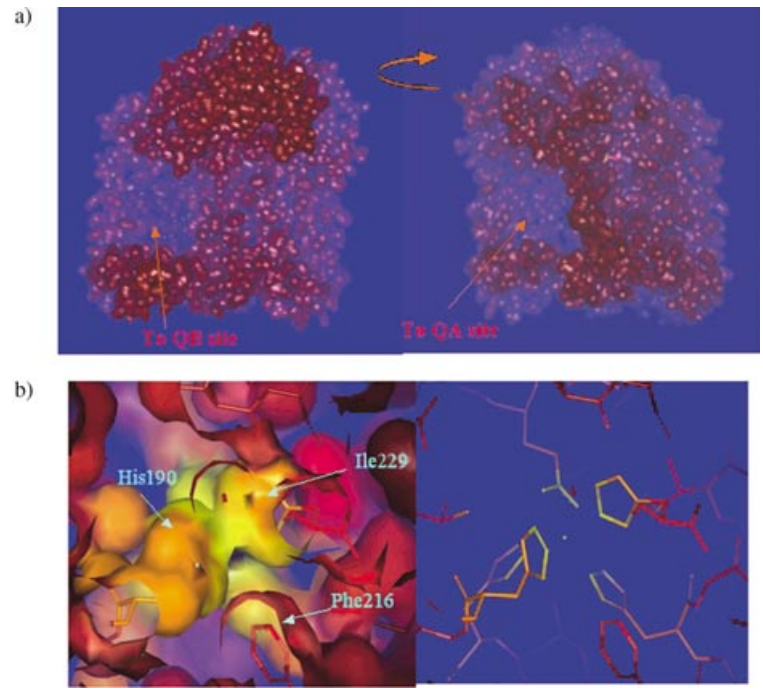

Figure 5. *a) Two global views, rotated by 180 degrees with respect to one another, of the van der Waals surface of the bacterial reaction center. b) Detail of the region near the Fe^{2+} ion, on the side of the Q_B site, where in the left part colors range from yellow to dark brown (through orange and red) with increasing distance from the iron center.*

the Q_B site of the reaction center, where the herbicide molecule may place itself. This space would even enlarge if the isoleucine at position 229 was free to move; interestingly, this residue has been shown, in *Rhodobacter sphaeroides*, to be involved in a mutation leading to herbicide resistance.[45] Moreover, the observed paramagnetic shifts caused by the iron center confirm its proximity to the herbicide.

Three main families of structures are found (shown in Figure 4a–c), one of which (b) places the carboxylate group of the herbicide near the iron center and could thus be stabilized by electrostatic interaction. Actually, no interaction was found at low pH values (data not shown) where the protonation of this moiety could weaken the binding. However, the absence of paramagnetic effects under these conditions could be due to the low stability and/or precipitation of the reaction center at low pH values. Another interesting feature is that acifluorfen is placed halfway between the iron and Q_B centers and could therefore act to block the electron transfer from Q_A to Q_B.

These findings are confirmed by the results of a docking calculation on the same system (data not shown), although the latter places the herbicide farther from the metal than expected from the experimental data. The reason is likely to be the one already mentioned with regard to the structure calculation with DYANA, that is, the protein was also kept fixed in the docking calculation and side-chain rearrangements of residues surrounding the Q_B site, in particular Ile229, were not allowed.

For paraquat the structure calculation with DYANA is meaningless, since this molecule, due to its symmetry, contains several protons that are quite far from each other but that give rise to indistinguishable signals; these, therefore, also give distance constraints that are averages of the real ones for the single protons. In this case we only performed a docking calculation, in order to see if the experimental distances were compatible with a model of the interaction based on theoretical affinity potentials for the various types of atoms. The results (Figure 6) show possible structures on two opposite sides with respect to the iron center and its ligands; these correspond to the Q_A and Q_B sites of the BRC.

Judging from the distances in Table 3, paraquat approaches the iron center with the methyl part first (this is indicated to be the nearest); among the families of structures found, the third one (Figure 6c) is in the best agreement with this, a result suggesting that paraquat would prefer the Q_B site (Figure 6a–c) to the Q_A site (Figure 6d). The location of paraquat in the Q_B site is confirmed independently by the fact that the

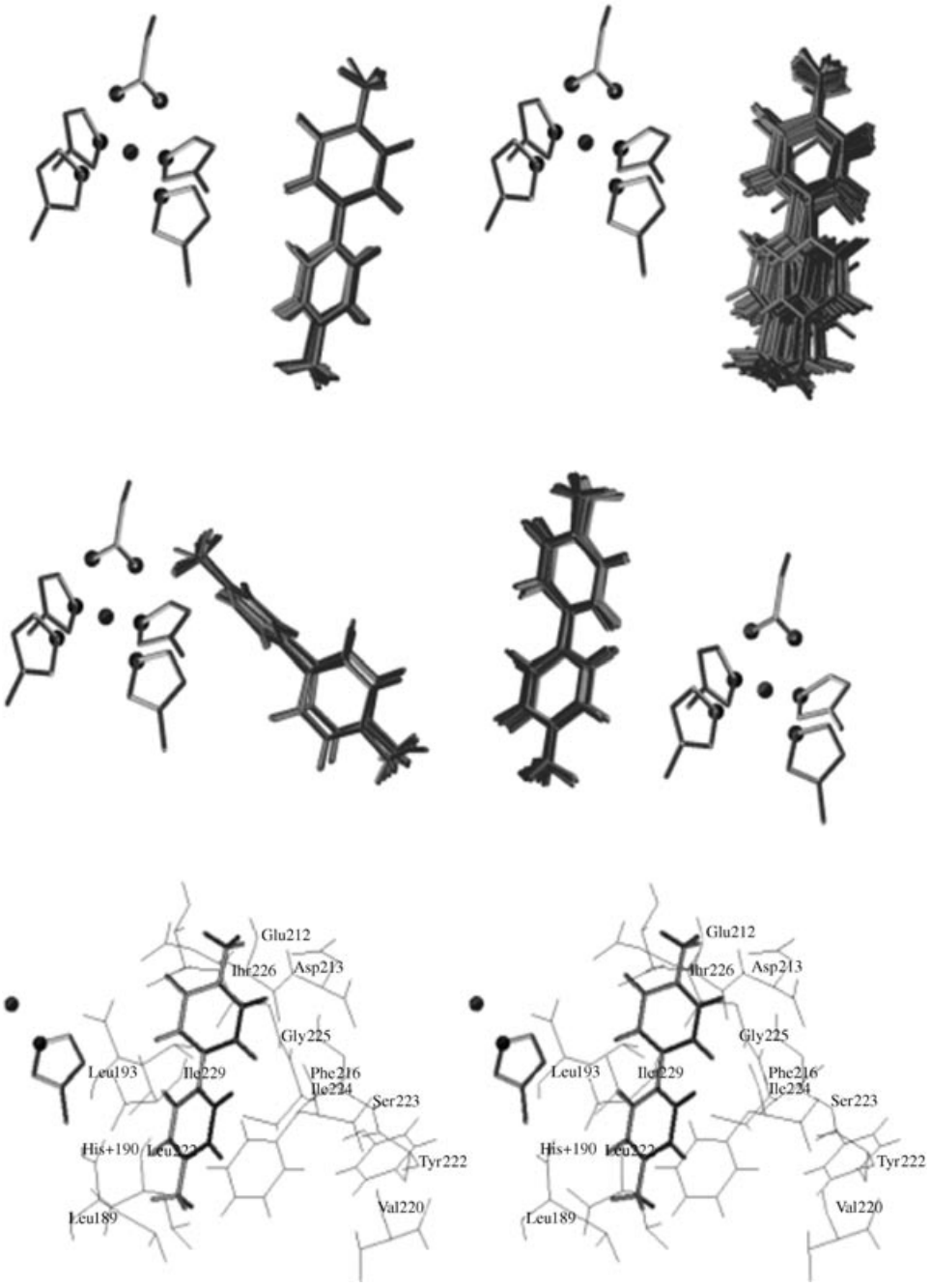

Figure 6. *Results of the docking calculation for paraquat and the BRC. a–d) The four families of conformations found. The orientation is the same as in Figure 4. e) The stereoview of the best structure (in terms of energy) for paraquat bound on the Q_B site is shown with the surrounding residues of the reaction center.*

three lowest energy structure families obtained by the docking calculation (Figure 6a–c), where no experimental constraints were included, all place the herbicide in this site. Actually, the quinone in the Q_A site is more tightly bound and more difficult to displace.[1,18] Also, this location of the paraquat molecule in the Q_B site (Figure 6a–c) strongly resembles that found for other herbicides and for the quinone Q_B,[4,8,12,16,17] being surrounded by the same amino acids. This is shown in Figure 6e, which represents a stereoview of the lowest energy structure (Figure 6a), with the surrounding residues of the reaction center. In particular, the polar and acidic moieties of the L subunit (such as SerL223, AspL213, and GluL212) which should be involved in the proton transfer into the Q_B binding site[46] find no oxygen to protonate; this could prevent the photosynthetic reaction.

Conclusion

The interaction of the two herbicides under examination, acifluorfen (ACF) and paraquat (PAR), with the photosynthetic reaction center from *Rhodobacter sphaeroides* has been investigated through NMR relaxation measurements. The interaction has been demonstrated by evaluating motional features of the bound form through cross-relaxation terms of protons at fixed distance on the herbicides, while paramagnetic contributions to relaxation rates of the herbicide protons, induced by the high-spin nonheme Fe^{II} ion in the BRC, have been converted into metal–proton distance constraints in order to obtain a model of the protein–herbicide adduct. The models place both herbicides in the vicinity of the Fe^{II} ion. In particular, ACF is located halfway between the metal and the Q_B site, a result explaining its blocking action on the electron transfer between the quinones in the Q_A and Q_B sites. For PAR the presence of pairs of undistinguishable protons far from each other prevents this direct procedure; however the comparison of a docking calculation with experimentally obtained distances leads to the conclusion that this molecule prefers the Q_B site to the Q_A site, a conclusion in agreement with the fact that the former is known to be more easily displaced by electron-transfer-blocking substances.

Experimental Section

Acifluorfen and paraquat were purchased from Supelco Inc. and were dissolved at basic pH values in D_2O and H_2O, respectively, without further purification. The pH value was then adjusted to 6.5 with DCl in the case of acifluorfen and to 6.9 with HCl for paraquat.

Bacterial reaction center preparations from *Rhodobacter sphaeroides* were obtained as described elsewhere.[47,48] After extraction and purification the BRCs were dialyzed against TLE buffer comprising 0.1% *n*-dodecyldimethylamine *N*-oxide (LDAO), 15 mM tris(hydroxymethyl)aminomethane (Tris)/HCl (pH 8), and 1 mM ethylenediaminetetraacetate (EDTA). The obtained ratio of the optical absorbance at 280/802 nm was 1.20 for the pure BRC preparation. The BRCs were concentrated by membrane filtration (Amicon Centricon 30) to a final concentration of 1.6 mM, as determined by the optical absorption at 802 nm.

NMR spectra were performed at 14.1 *T* with a Bruker Avance 600 MHz spectrometer at controlled temperatures (298 ± 0.1 K). Chemical shifts were referenced to [$^2H_4$]-trimethylsilylpropanesulfonate ([D_4]TSP). The assignment was accomplished with COSY and NOESY 2D experiments. NOESY spectra were obtained with standard pulse sequences and mixing-time values of 50–350 ms. During all 2D experiments, water suppression was achieved by means of the presaturation or excitation-sculpting method.[49]

Spin-lattice relaxation rates were measured with inversion-recovery pulse sequences. The same sequence was also used to measure the single- or double-selective relaxation rates by means of suitably shaped π pulses, generated by the SHAPE TOOL module of the Bruker program XWINNMR, instead of the usual nonselective π pulse. All rates were calculated by regression analysis of the initial recovery curves of longitudinal magnetization components and had errors not larger than ± 3%.

T_1 values were converted into distance constraints as described in the Results and Discussion section. Simulated annealing in the torsional angle space was performed by using the PSEUDYANA[50] module of the program DYANA,[44] with 10000 steps and 300 random starting positions of the herbicide generated by the program itself around the bacterial reaction center X-ray diffraction structure,[8] from which we removed the two quinones because quinone Q_B is known to be displaced by a series of herbicides.

Docking calculations were performed with the program AutoDock 3.0.[51–53] A grid of 120 elements for each direction with a spacing of 0.375 Å was used, centered near the iron atom. The calculations were performed by using the Lamarckian genetic algorithm. A population of 100 individuals was used, of which the best 10 in terms of energy survived at each generation, with a gene mutation rate of 0.02, a crossover rate of 0.80, a maximum of 250000 energy evaluations and of 27000 generations, and a total of 256 runs. In this case we also removed the two quinones from the BRC structure.

Protein charges were assigned according to the GROMOS force field,[54] with a +2 charge assigned to the Fe ion, while partial charges of paraquat atoms were determined through an ab initio calculation with the program GAUSSIAN98[55] by using the natural bond orbital (NBO) procedure. The calculation was performed with the restricted Hartree–Fock (RHF) method, by using the 6–31g(d,p) basis for all atoms.

Acknowledgements

The authors wish to thank C. Schulz (TU Berlin, Germany), F. Milano (University of Bari, Italy), and F. Berti (Chiron Spa, Siena, Italy) for the preparation of the reaction centers. The work of E.M. was supported by the CIRMMP (Consorzio Interuniversitario Risonanze Magnetiche di Metalloproteine Paramagnetiche).

Keywords: electron transfer · herbicides · NMR spectroscopy · photosynthesis · structure–activity relationships

[1] W. Vermaas, *Annu. Rev. Plant Physiol. Plant Mol. Biol.* **1993**, *44*, 457–481.
[2] A. Zouni, H. T. Witt, J. Kern, P. Fromme, N. Krauss, W. Saenger, P. Orth, *Nature* **2001**, *409*, 739–743.
[3] N. Kamiya, J. R. Shen, *Proc. Natl. Acad. Sci. USA* **2003**, *100*, 98–103.
[4] C. R. D. Lancaster, U. Ermler, H. Michel in *Advances in Photosynthesis: Anoxygenic Photosynthetic Bacteria* (Eds.: R. E. Blankenship, M. T. Madigan,

C. E. Bauer), Kluwer Academic Publishers, Dordrecht, The Netherlands, **1995**, pp. 503 – 526.
[5] A. Kuglstatter, U. Ermler, H. Michel, L. Baciou, G. Fritzsch, *Biochemistry* **2001**, *40*, 4253 – 4260.
[6] B. Hankamer, E. Morris, J. Nield, C. Gerle, J. Barber, *J. Struct. Biol.* **2001**, *135*, 262 – 269.
[7] E. P. Morris, B. Hankamer, D. Zheleva, G. Friso, J. Barber, *Structure* **1997**, *5*, 837 – 849.
[8] M. H. Stowell, T. M. McPhillips, D. C. Rees, S. M. Soltis, E. Abresch, G. Feher, *Science* **1997**, *276*, 812 – 816.
[9] H. Michel, J. Deisenhofer, *Biochemistry* **1988**, *27*, 1 – 7.
[10] J. P. Allen, G. Feher, T. O. Yeates, D. C. Rees, J. Diesenhofer, H. Michel, R. Huber, *Proc. Natl. Acad. Sci. USA* **1986**, *83*, 8589 – 8593.
[11] C. H. Chang, D. Tiede, J. Tang, U. Smith, J. Norris, M. Schiffer, *FEBS Lett.* **1986**, *205*, 82 – 86.
[12] U. Ermler, G. Fritzsch, S. K. Buchanan, H. Michel, *Structure* **1994**, *2*, 925 – 936.
[13] I. Sinning, *Trends Biochem. Sci.* **1992**, *17*, 150 – 154.
[14] C. R. D. Lancaster, H. Michel, *Structure* **1997**, *5*, 1339 – 1359.
[15] M. L. Paddock, S. H. Rongey, E. C. Abresch, G. Feher, M. Y. Okamura, *Photosynth. Res.* **1998**, *17*, 75 – 96, and references therein.
[16] G. Feher, M. Y. Okamura, *Appl. Magn. Reson.* **1999**, *16*, 63 – 100.
[17] C. R. D. Lancaster, H. Michel, *J. Mol. Biol.* **1999**, *286*, 883 – 898.
[18] O. El-Kabbani, C. H. Chang, D. Tiede, J. Norris, M. Schiffer, *Biochemistry* **1991**, *30*, 5361 – 5369.
[19] E. Frolov, A. Birk, G. Fritzsch, I. Sinning, H. Michel, V. I. Goldanskii, F. Parak, *Hyperfine Interactions* **1991**, *68*, 59 – 70.
[20] J. S. van den Brink, T. E. P. Hermolle, P. Gast, P. J. Hore, A. J. Hoff, *J. Phys. Chem.* **1996**, *100*, 2430 – 2437.
[21] A. Remy, R. B. Boers, T. Egorova-Zachernyuk, P. Gast, J. Lugtenburg, K. Gerwert, *Eur. J. Biochem.* **2003**, *270*, 3603 – 3609.
[22] C. R. D. Lancaster, *Biochem. Soc. Trans.* **1999**, *27*, 591 – 596.
[23] U. Egner, G. A. Hoyer, W. Saenger, *Eur. J. Biochem.* **1992**, *206*, 685 – 690.
[24] I. Sinning, *Photosynth. Res.* **1992**, *34*, 97 – 97.
[25] N. Ginet, J. Lavergne, *Biochemistry* **2001**, *40*, 1812 – 1823.
[26] R. R. Stein, A. L. Castellvi, J. P. Bogacz, C. A. Wraight, *J. Cell. Biochem.* **1984**, *24*, 243 – 259.
[27] P. Böger, K. Wakabayashi, *Z. Naturforsch. C: Biosci.* **1995**, *50c*, 159 – 166.
[28] P. Böger, K. Wakabayashi, *Z. Naturforsch. C: Biosci.* **1995**, *50c*, 591 – 601.
[29] F. Berti, E. Gaggelli, G. Valensin, *Appl. Magn. Reson.* **2000**, *18*, 289 – 301.
[30] D. J. Gillham, A. D. Dodge, *Pestic. Sci.* **1987**, *19*, 25 – 34.
[31] I. Gupta, B. C. Tripathy, *Indian J. Biochem. Bio.* **2000**, *37*, 498 – 505.
[32] P. Slade, A. Calderblank in *Herbicides: Chemistry, Degradation and Mode of Action* (Eds.: P. C. Keamey, D. D. Kaufman), 2nd ed., Marcel Dekker, New York, **1975**, Chapter 10.
[33] G. Valensin, T. Kushnir, G. Navon, *J. Magn. Reson.* **1982**, *46*, 23 – 29.
[34] I. Barni Comparini, E. Gaggelli, N. Marchettini, G. Valensin, *Biophys. J.* **1985**, *48*, 247 – 251.
[35] E. Gaggelli, N. Gaggelli, A. Maccotta, G. Valensin, *J. Magn. Reson. B* **1994**, *104*, 89 – 94.
[36] I. Bertini, C. Luchinat, *Coord. Chem. Rev.* **1996**, *150*.
[37] I. Bertini, C. Luchinat, *NMR of Paramagnetic Molecules in Biological Systems*, Benjamin/Cummings, Menlo Park, CA, **1986**.
[38] S. Aime, N. D'Amelio, M. Fragai, Y. M. Lee, C. Luchinat, E. Terreno, G. Valensin, *J. Biol. Inorg. Chem.* **2002**, *7*, 617 – 622.
[39] G. H. Lee, *J. Agric. Food Chem.* **1985**, *33*, 499 – 503.
[40] *Handbook of Chemistry and Physics. A Ready-Reference Book of Chemical and Physical Data*, 52nd ed., (Ed.: R. C. Weast), The Chemical Rubber Company, Cleveland, OH, **1971**.
[41] J. Cavanagh, W. J. Fairbrother, A. G. Palmer III, N. J. Skelton, *Protein NMR Spectroscopy: Principles and practice*, Academic Press, San Diego, CA, **1996**.
[42] F. Lendzian, W. Lubitz, H. Scheeer, C. Bubenzer, K. Möbius, *J. Am. Chem. Soc.* **1981**, *103*, 4635 – 4637.
[43] R. Calvo, R. A. Isaacson, E. C. Abresch, M. Y. Okamura, G. Feher, *Biophys. J.* **2002**, *83*, 2440 – 2456.
[44] P. Güntert, C. Mumenthaler, K. Wüthrich, *J. Mol. Biol.* **1997**, *273*, 283 – 298.
[45] M. L. Paddock, J. C. William, S. Rongey, E. C. Abresch, G. Feher in *Progress in Photosynthesis Research, Vol. 111* (Ed.: J. Biggins), Martinus, Nijholt-Dordrecht, The Netherlands, **1987**, pp. 775 – 778.
[46] M. Y. Okamura, M. L. Paddock, M. S. Graige, G. Feher, *Biochim. Biophys. Acta* **2000**, *1458*, 148 – 163.
[47] J. Rautter, F. Lendzian, C. Schulz, A. Fetsch, M. Kuhn, X. Lin, J. C. Williams, J. P. Allen, W. Lubitz, *Biochemistry* **1995**, *34*, 8130 – 8143.
[48] G. Feher, M. Y. Okamura in *The Photosynthetic Bacteria* (Eds.: R. K. Clayton, W. R. Sistrom), Plenum Press, New York, **1978**, pp. 349 – 386.
[49] T. L. Hwang, A. J. Shaka, *J. Magn. Reson. A* **1995**, *112*, 275 – 279.
[50] L. Banci, I. Bertini, M. A. Cremonini, G. Gori Savellini, C. Luchinat, K. Wüthrich, P. Güntert, *J. Biomol. NMR* **1998**, *12*, 553 – 557.
[51] D. S. Goodsell, A. J. Olson, *Proteins Struct. Funct. Genet.* **1990**, *8*, 195 – 202.
[52] G. M. Morris, D. S. Goodsell, R. Huey, A. J. Olson, *J. Computer-Aided Mol. Design* **1996**, *10*, 293 – 304.
[53] G. M. Morris, D. S. Goodsell, R. S. Halliday, R. Huey, W. E. Hart, R. K. Belew, A. J. Olson, *J. Comput. Chem.* **1998**, *19*, 1639 – 1662.
[54] W. F. Van Gunsteren, X. Daura, A. E. Mark in *Encyclopedia of Computational Chemistry, Vol. 2* (Eds.: P. von Ragué Schleyer, P. R. Schreiner), Wiley, Chichester, **1998**.
[55] *Gaussian 98 (Revision A.3)*, M. J. Frisch, G. W. Trucks, H. B. Schlegel, G. E. Scuseria, M. A. Robb, J. R. Cheeseman, V. G. Zakrzewski, J. A. Montgomery, Jr., R. E. Stratmann, J. C. Burant, S. Dapprich, J. M. Millam, A. D. Daniels, K. N. Kudin, M. C. Strain, O. Farkas, J. Tomasi, V. Barone, M. Cossi, R. Cammi, B. Mennucci, C. Pomelli, C. Adamo, S. Clifford, J. Ochterski, G. A. Petersson, P. Y. Ayala, Q. Cui, K. Morokuma, D. K. Malick, A. D. Rabuck, K. Raghavachari, J. B. Foresman, J. Cioslowski, J. V. Ortiz, B. B. Stefanov, G. Liu, A. Liashenko, P. Piskorz, I. Komaromi, R. Gomperts, R. L. Martin, D. J. Fox, T. Keith, M. A. Al-Laham, C. Y. Peng, A. Nanayakkara, C. Gonzalez, M. Challacombe, P. M. W. Gill, B. G. Johnson, W. Chen, M. W. Wong, J. L. Andres, M. Head-Gordon, E. S. Replogle, J. A. Pople, Gaussian, Inc., Pittsburgh, PA, **1998**.

Received: January 16, 2004

